

Impact of palladium silicide formation on the catalytic properties of Pd/SiO₂ catalysts in liquid-phase semihydrogenation of phenylacetylene

Joongjai Panpranot^{a,*}, Kunnika Phandinthong^a, Terachai Sirikajorn^a,
Masahiko Arai^b, Piyasan Praserttham^a

^a Center of Excellence on Catalysis and Catalytic Reaction Engineering, Department of Chemical Engineering,
Faculty of Engineering, Chulalongkorn University, Bangkok 10330, Thailand

^b Division of Chemical Process Engineering, Graduate School of Engineering, Hokkaido University, Sapporo, Japan

Received 18 May 2006; received in revised form 19 July 2006; accepted 19 July 2006

Available online 1 September 2006

Abstract

In this study, palladium silicide was formed on the sol–gel derived SiO₂ supported Pd catalysts when they were prepared by ion-exchange method using Pd(NH₃)₄Cl₂ as a palladium precursor. No other palladium phases (PdO or Pd⁰) were evident after calcinations at 450 °C for 3 h. The Pd/SiO₂ catalysts with Pd silicide formation were found to exhibit superior performance than commercial SiO₂ supported ones in liquid-phase semihydrogenation of phenylacetylene. From XPS results, the binding energy of Pd 3d of palladium silicide on the Pd/SiO₂ catalyst shifted toward larger binding energy, indicating that Pd is electron deficient. This could probably result in an inhibition of a product styrene on the Pd surface and hence high styrene selectivities were obtained at high phenylacetylene conversions. The formation of Pd silicide, however, did not have much impact on specific activity of the Pd catalysts since the TOFs were quite similar among the various catalysts with or without palladium silicides if their average particle sizes were large enough. The TOFs decreased by an order of magnitude when palladium dispersion was very high and their average particle sizes were smaller than 3–5 nm.

© 2006 Elsevier B.V. All rights reserved.

Keywords: Palladium silicide; Pd/SiO₂; Sol–gel silica; Liquid-phase hydrogenation; Phenylacetylene

1. Introduction

Pd/SiO₂ is one of the most frequently studied catalysts for liquid-phase alkyne semihydrogenation [1–8]. It is also commercially attractive for industrial applications due to its easy preparation procedure and low separation problem compared to colloiddally dispersed ones. SiO₂ is a common support and known to be more inert than several reducible metal oxides such as TiO₂ or CeO₂ [9]. However, Pd–SiO₂ interaction can occur under certain cases, e.g., high temperature treatment in the presence of H₂ [10,11]. This transformation has been shown to alter the catalytic behavior of reduced Pd/SiO₂ catalysts. For example, in catalytic conversion of 2,2-dimethylbutane, formation of palladium silicides lowered the catalytic activity, decreased the activation energy, and increased the selectivity

toward isomerization reaction [10]. Although metal silicide formation seemed to be a problem in catalysis on supported metal, there has been a number of studies reporting the application of palladium silicon alloy in catalytic reactions [12–14]. For instance, Baiker and coworkers [14] reported that the amorphous glassy alloy Pd₈₁Si₁₉ prepared by melt spinning was suitable for semihydrogenation of a propargylic alcohol and exhibited more than 50 times higher turnover frequency than a conventional silica-supported palladium catalyst under similar conditions.

In this study, palladium silicide was formed on sol–gel derived nano-SiO₂ supported Pd catalysts via a simple ion-exchange method. No high temperature reduction treatment was required for such formation. The catalysts were investigated by means of N₂ physisorption, CO pulse chemisorption, X-ray diffraction (XRD), transmission electron microscopy (TEM), and X-ray photoelectron spectroscopy (XPS). The effects of preparation method as well as the type of silica support on the characteristics and catalytic properties of Pd/SiO₂

* Corresponding author. Tel.: +66 2218 6878; fax: +66 2218 6877.
E-mail address: joongjai.p@eng.chula.ac.th (J. Panpranot).

were extensively investigated in selective hydrogenation of phenylacetylene in a liquid–solid–gas system.

2. Experimental

2.1. Catalyst preparation

Silica was prepared by the sol–gel technique using the sol composition of 40 ml of tetraethylorthosilicate (TEOS), 10.5 ml of ethanol, 12.5 ml of de-ionized water, and 1 ml of hydrochloric acid (HCl). The mixtures were stirred vigorously for 1 h. Then the gel was calcined at 500 °C for 6 h in order to remove any organic. For comparison purposes, commercial silica was large-pore silica obtained from Strem Chemicals. The Pd/SiO₂ catalysts with ca. 1 wt.% of Pd were prepared by ion-exchange and impregnation methods. For the ion-exchange method, a desired amount of Pd(NH₃)₄Cl₂ (Aldrich) was dissolved in de-ionized water. The pH of solution was adjusted to 12 using 25% NH₃ solution (Aldrich). The precursor solution was added to the silica and stirred vigorously for 3 days. The residue solid was filtered and washed with distilled water until the pH was 7. For incipient wetness impregnation method, the silica support was impregnated with an aqueous solution containing certain amount of palladium. The catalyst samples were dried in oven at 100 °C and calcined in air at 450 °C for 3 h prior to characterization.

2.2. Catalyst characterization

The BET surface areas, pore volumes, and average pore diameters were determined by N₂ physisorption using a Micromeritics ASAP 2000 automated system. Each sample was degassed under vacuum at <10 μmHg in the Micromeritics ASAP 2000 at 150 °C for 4 h prior to N₂ physisorption. The XRD patterns of the catalysts were measured from 20 to 80° 2θ using a SIEMENS D5000 X-ray diffractometer and Cu Kα radiation with a Ni filter. Catalyst crystallite sizes and diffraction pattern of silica supports were obtained using the JEOL JEM 2010 transmission electron microscope that employed a LaB₆ electron gun in the voltage range of 80–200 kV with an optical point to point resolution of 0.23 nm. The amounts of CO chemisorbed on the catalysts were measured using a Micromeritic Chemisorb 2750 automated system attached with ChemiSoft TPx software at room temperature. Prior to chemisorption, the sample was reduced in a H₂ flow at 500 °C for 2 h and then cooled down to ambient temperature in a He flow. The XPS analysis was performed using an AMICUS photoelectron spectrometer equipped with a Mg Kα X-ray as a primary excitation and a KRATOS VISION2 software. XPS elemental spectra were acquired with 0.1 eV energy step at a pass energy of 75 kV. The C 1s line was taken as an internal standard at 285.0 eV.

2.3. Reaction study

Liquid-phase semihydrogenation of phenylacetylene was carried out in a 50 cm³ stainless steel autoclave. Approximately 0.1 g of Pd/SiO₂ catalyst was placed in the reactor with 1 cm³

of phenylacetylene and 9 cm³ of ethanol (Aldrich). Afterward the reactor was filled with hydrogen at 1 bar pressure. Stirring was switched on to start the reaction and carried out for 1 h. The products were analyzed by gas chromatography with flame ionized detector.

3. Results and discussion

3.1. Catalyst characterization

3.1.1. TEM with electron diffraction mode

Transmission electron micrographs and electron diffraction patterns of the two types of the SiO₂ used in this study namely SiO₂-SG (sol–gel derived silica) and SiO₂-com (commercial silica) are shown in Fig. 1. The TEM images revealed that the commercial silica is composed of many small particles with an average particle size of ca. 17 nm while larger particle size was seen for the sol–gel derived silica. However, sol–gel method usually produces single crystalline oxides, the large particles observed maybe the secondary particles formed by agglomeration of the primary nano-particles due to heat treatment during calcination step. Electron diffraction pattern of the commercial silica is clear indicating that it is totally amorphous while that of the sol–gel derived silica indicated semi-polycrystalline structure.

3.1.2. N₂ physisorption

The BET surface areas, the pore volumes, and the average pore diameters of the silica and the silica-supported Pd catalysts are shown in Table 1. The catalysts were termed Pd/SiO₂-*x*-im and Pd/SiO₂-*x*-ion according to the two preparation methods used where *x* = sol–gel derived (SG) or commercial SiO₂ (com). The N₂ adsorption–desorption isotherms of the sol–gel derived nano-silica and the commercial silica (not shown) indicate a typical type IV isotherm with a sharp inflection at relative pressure $P/P_0 > 0.3$, characteristics of capillary condensation. After Pd loading by the impregnation method, the BET surface areas and pore volumes slightly decreased (less than 20%) indicating that only a small amount of Pd was deposited in the pores of the silica. In contrast, the BET surface areas and pore volumes of the Pd/SiO₂ catalysts prepared by ion-exchange method dramatically decreased (~95%). Such results suggest that pore blockage or destruction of the silica pore structure occurred in such cases. There were no changes in the average pore diameters of both types of silica when the catalysts were prepared by impregnation method. It did appreciably change for those prepared by ion-exchange method.

3.1.3. X-ray diffraction

The XRD patterns of the various Pd/SiO₂ catalysts prepared by impregnation and ion-exchange method in the calcined state are shown in Fig. 2. The XRD characteristic peaks for PdO at 2θ (°) = 33.8, and less so at 42.0, 54.8, 60.7, and 71.4 were evident only for the catalysts prepared by impregnation method with Pd/SiO₂-SG-im exhibited higher peak intensities. The average PdO crystallite sizes on SiO₂-SG-im and SiO₂-com-im

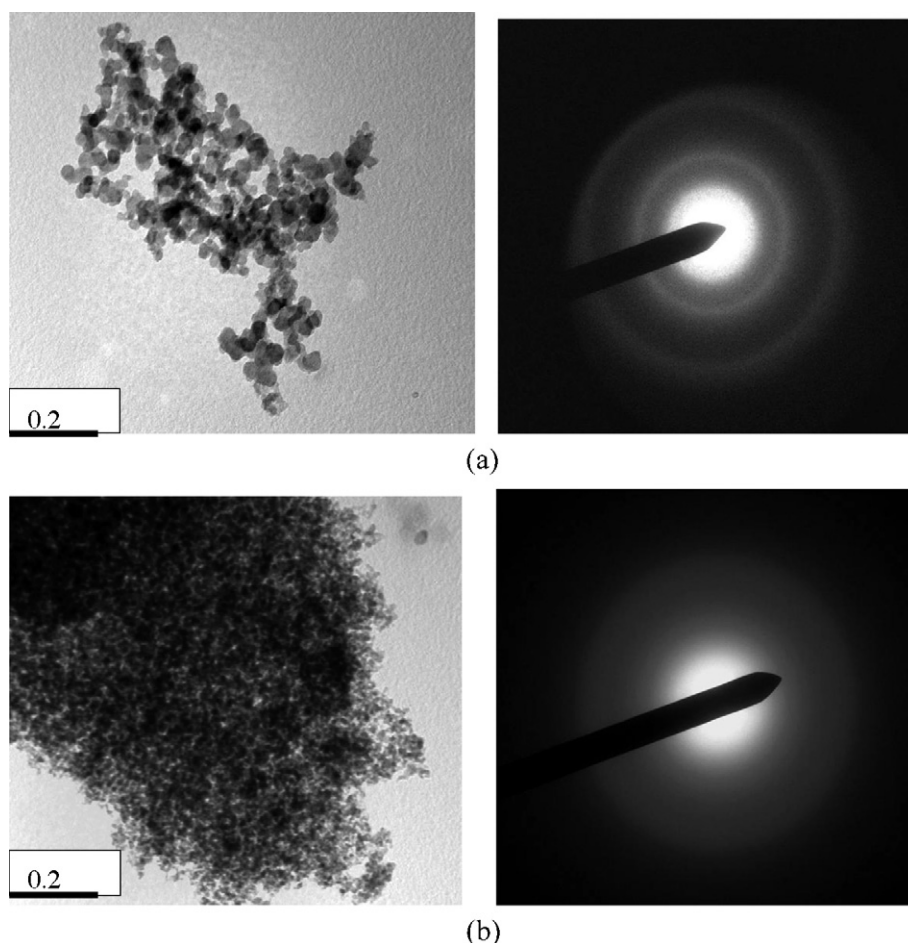


Fig. 1. TEM micrographs and diffraction patterns of (a) SiO₂-SG and (b) SiO₂-com.

were calculated from the full width at half maximum of the XRD peak at $2\theta = 33.8^\circ$ using Scherrer equation to be 9.6 and 11.4 nm, respectively (Table 2). For the catalysts prepared by ion-exchange method, it was found that palladium silicide was formed on the sol-gel derived silica as indicated by the major XRD characteristic peak for Pd₄Si at $2\theta = 18.1^\circ$. The average crystallite size of palladium silicide was calculated to be ca. 60 nm. It should be noted that there was no XRD characteristic peak of palladium silicide for the commercial silica supported Pd catalyst prepared by the ion-exchange method. In such case, Pd was probably highly dispersed and its average particle size was smaller than the detectability limit of the XRD (3–5 nm).

3.1.4. Surface analysis by XPS

Because of its surface sensitivity, XPS is used to identify the surface compositions of the catalysts as well as the interaction between Pd and the silica supports. The percentages of atomic concentration for Si 2p, O 1s, and Pd 3d are given in Table 2. There was a significant difference in the atomic ratios of Si/Pd for the sol-gel derived silica supported Pd catalysts prepared by impregnation and ion-exchange methods (19 and 215, respectively). While those for the commercial silica supported ones were ca. 300 and 400 for the ones prepared by impregnation and ion-exchange, respectively. The low Si/Pd ratio found for Pd/SiO₂-SG-im catalyst suggests that large amount of palladium

Table 1
N₂ physisorption results

Sample	N ₂ physisorption		
	BET surface area (m ² /g)	Pore volume (cm ³ /g)	Average pore diameter (nm)
SiO ₂ -SG	307.2	0.145	1.9
SiO ₂ -com	243.8	1.060	17.4
Pd/SiO ₂ -SG-im	248.0	0.118	1.9
Pd/SiO ₂ -com-im	234.0	1.017	17.3
Pd/SiO ₂ -SG-ion	6.2	0.009	5.9
Pd/SiO ₂ -com-ion	5.5	0.041	29.5

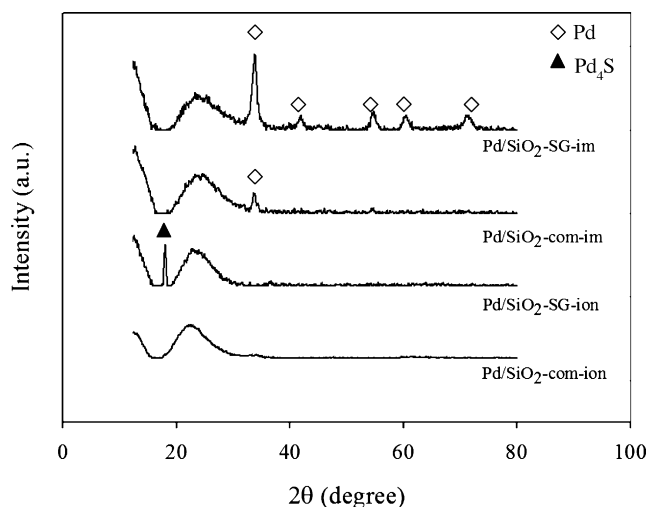


Fig. 2. XRD patterns of the various SiO₂ supported Pd catalysts.

existed on the outside of the support surface and not in the pores; the results were consistent with the N₂ physisorption results that the average pore diameters remained unaltered (~1.9 nm before and after Pd impregnation). The higher Si/Pd ratios for the other catalysts suggest that most of the palladium existed deep inside the pore of the supports rather than on the outer surface. This could be the case for the large pore commercial silica supported ones since the pores were large enough so that the solution of Pd precursor could easily be absorbed during the preparation using either impregnation or ion-exchange method. However, for the sol-gel derived silica, the pores were so small that the preparation solution could hardly penetrate these pores. The enrichment of Si component on the surface of the Pd/SiO₂-SG-ion was due to palladium silicide formation as shown earlier in its XRD pattern. A large number of the Si/Pd atomic ratio due to palladium silicide formation has also been reported for amorphous Pd₈₁Si₁₉ alloy catalysts [13].

The elemental scans for each component on the surfaces of the SiO₂ and the SiO₂ supported Pd catalysts prepared by impregnation and ion-exchange are shown in Figs. 3–5, respectively. For the silica supports, it was found that the binding energies of both Si 2p and O 1s for the sol-gel derived SiO₂ shifted towards lower binding energies. This suggest that on the sol-gel derived SiO₂ the Si–O–Si matrix may become the non-stoichiometric SiO_x (0 < x < 2) upon preparation by sol-gel technique and subsequent calcinations at high temperature. These defective sites of the SiO₂ have been found to lower the binding energy of

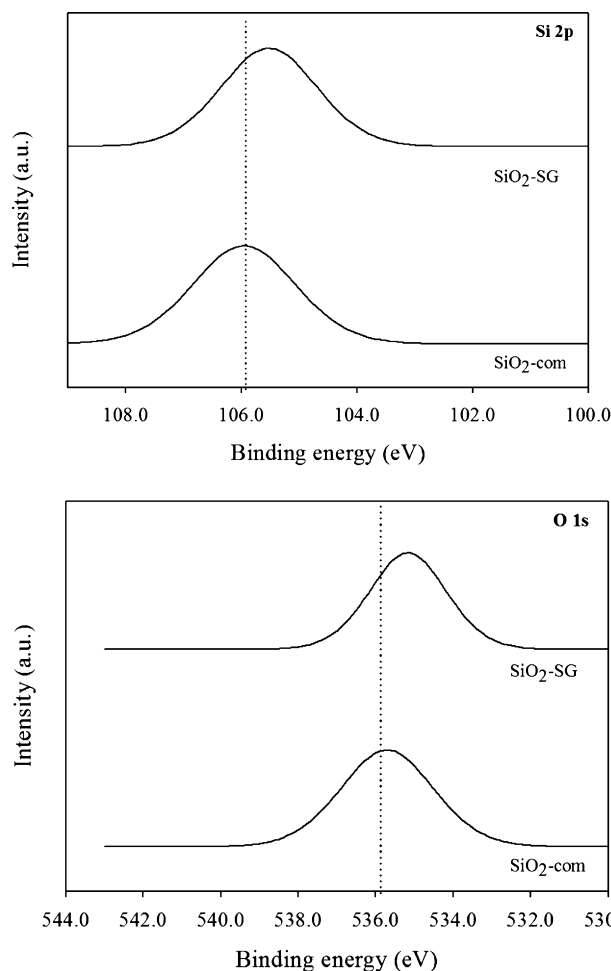


Fig. 3. XPS results of SiO₂-SG and SiO₂-com.

both Si 2p and O 1s [15]. For the Pd/SiO₂ catalysts prepared by impregnation method, there were no changes for the binding energies of Si 2p and O 1s for both Pd/SiO₂-SG-im and Pd/SiO₂-com-im. The binding energies of Pd 3d for both catalysts were also identical. Such results indicate that there was no interaction between Pd and the SiO₂ supports when the catalysts were prepared by impregnation method. On the other hand, for those prepared by ion-exchange method, the binding energies of Si 2p, O 1s, and Pd 3d for Pd/SiO₂-SG-ion shifted towards higher binding energies while those of Pd/SiO₂-com-ion were essentially the same. It is likely that formation of palladium silicide on the Pd/SiO₂-SG-ion resulted in a stronger interaction between Pd and SiO₂.

Table 2
Catalyst characterization by XRD and XPS

Catalyst	XRD		Atomic concentration (%)			Si/Pd
	Phase	Crystallite size (nm)	Si 2p	O 1s	Pd 3d	
Pd/SiO ₂ -SG-im	PdO	9.6	24.06	74.49	1.45	19.40
Pd/SiO ₂ -com-im	PdO	11.4	21.44	78.49	0.07	306.22
Pd/SiO ₂ -SG-ion	PdSi	61.2	25.80	74.09	0.12	215.00
Pd/SiO ₂ -com-ion	n.d.	n.d.	28.21	71.60	0.08	403.02

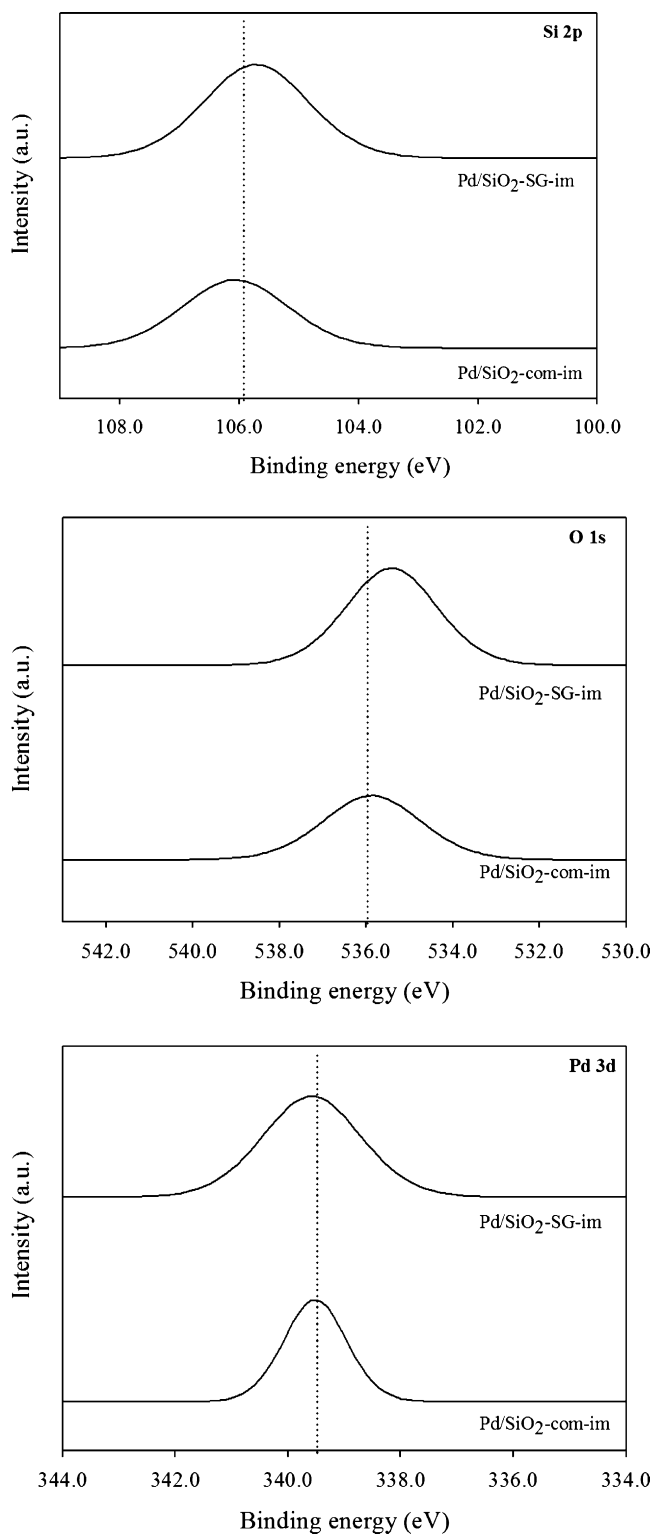


Fig. 4. XPS results of Pd/SiO₂-SG and Pd/SiO₂-com prepared by impregnation method.

3.2. Proposed mechanism for palladium silicide formation

Palladium silicides exist in various compositions such as Pd₂Si [16], Pd₃Si [11,17,18], Pd₄Si [18,19], or Pd₅Si [17]. Most of Pd silicide formation for Pd/SiO₂ catalysts reported in the lit-

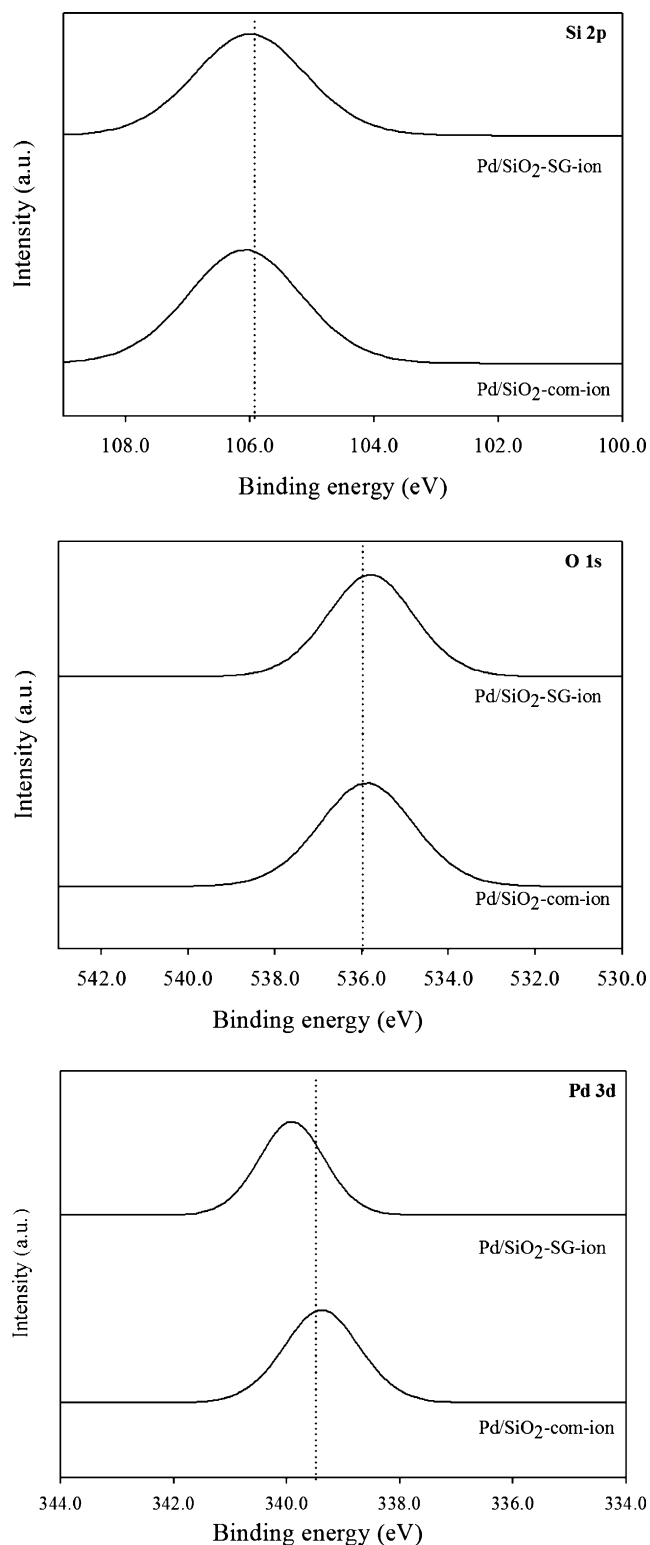


Fig. 5. XPS results of Pd/SiO₂-SG and Pd/SiO₂-com prepared by ion-exchange method.

erature resulted from a high temperature reduction treatment (450 °C and above) in the presence of hydrogen [13,14]. The mechanism of Pd-silicon interactions generated by high temperature reduction proposed by Karpinski and coworkers [18] involved incorporation of silicon into a palladium phase, not

Table 3
CO chemisorption results and catalyst activity in selective phenylacetylene hydrogenation

Catalyst	CO chemisorption ($\times 10^{-18}$ molecule CO/g _{cat})	Conversion ^a (%)	Selectivity ^a (%)		TOFs ^b (s ⁻¹)
			Styrene	Ethylbenzene	
Pd/SiO ₂ -SG-im	7.41	51.1	96.0	4.0	1.20
Pd/SiO ₂ -com-im	3.32	31.2	91.1	8.9	1.61
Pd/SiO ₂ -SG-ion	3.92	40.1	92.9	7.1	1.74
Pd/SiO ₂ -com-ion	46.8	54.8	88.5	11.5	0.20

^a The reaction conditions were H₂ 1 bar, 30 °C, and reaction time 1 h.

^b Based on CO chemisorption results.

vice versa. Reduction of Pd/SiO₂ at high temperature initially resulted in Pd₄Si formation which was then further reacted with silicon species to a Pd₃Si phase. Other possible mechanisms involved diffusion of Si through a thin layer of Pd to the surface [20–22]. However, in this study, formation of palladium occurred during preparation of sol–gel derived silica supported Pd catalysts by ion-exchange method following calcination at 450 °C for 3 h. The use of commercial amorphous SiO₂ did not result in such formation. Based on the work of Ichinohe et al. [15] about palladium silicide formation in Pd/SiO₂ complex films, it is believed that oxygen vacancies are the primary diffusion pathways for the formation of silicide at the interface between SiO₂ and Si. Point defects on SiO₂ thin film has been reported as the primary mechanism for inter-diffusion of Pd. Deposition of elemental Si on Pd on less defective SiO₂ thin film does not produce a silicide feature. The results in this study are in good agreement with those reports that palladium silicide formation was initiated from the defective sites of the SiO₂ since the sol–gel derived SiO₂ contained more defective sites than the commercial ones (as shown by a shift of the XPS Si 2p peak toward lower binding energy).

3.3. Catalyst activity in liquid phase hydrogenation of phenyl acetylene

Table 3 shows the CO chemisorption results, the activity and the selectivity of the catalysts in liquid phase hydrogenation of phenyl acetylene, and the calculated turnover frequencies (TOF). The effect of Pd dispersion on the alkyne hydrogenation has been widely studied and it is well known that changes in metal dispersion, i.e. different particle sizes lead to changes in TOF and selectivity. Since the catalyst activities/conversions in this study (e.g. for Pd/SiO₂-SG-ion and Pd/SiO₂-com-ion) did not correlate with the CO chemisorption results and only TOF was changed significantly. This indicates that the specific activity of such catalysts depends on the Pd particle size and the reaction may be a structure-sensitive reaction. Such results, however, were found to be in agreement with the well-established trend in the literature that the specific activity decreases as metal particle size decreases [23–29]. The difference becomes significant when the average Pd particle size is very small (<3–5 nm).

Overall, the selectivity for styrene of the sol–gel derived silica supported Pd catalysts was higher than those of the commercial silica supported ones regardless the preparation method used. From the performance curves of all the catalysts (Fig. 6), the

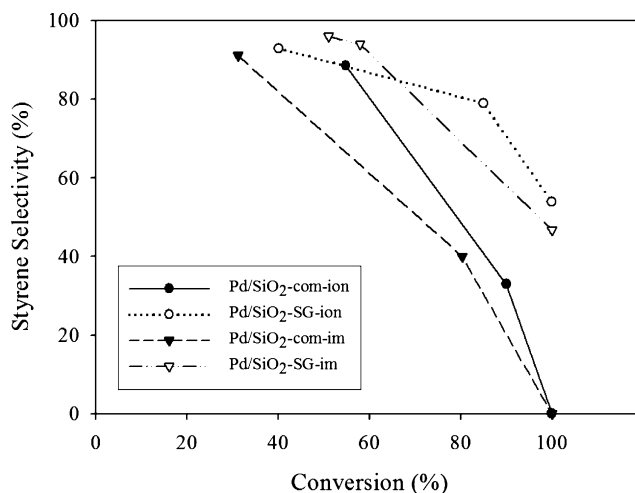


Fig. 6. Performance curves of Pd/SiO₂-SG and Pd/SiO₂-com catalysts.

sol–gel derived silica supported Pd catalysts prepared by ion-exchange and impregnation method exhibited relatively high styrene selectivity at 100% conversion of phenylacetylene with the one containing palladium silicide exhibited the highest selectivity. Under similar conditions, the commercial supported catalysts (both Pd/SiO₂-com-im and Pd/SiO₂-com-ion) exhibited no styrene selectivity at all. A possible explanation is an inhibition of a product of styrene, which is adsorbed on the surface of Pd, more strongly on Pd/SiO₂-SG in which Pd is electron-deficient (larger binding energy from XPS results). Additional hydrogenation reaction experiments with only styrene and the mixture of styrene and phenylacetylene were carried out in order to confirm the hypothesis. It was found that the commercial silica supported Pd catalysts exhibited higher styrene conversion than the sol–gel derived silica supported ones during hydrogenation of only styrene. Higher ethylbenzene selectivities were also observed for the commercial silica supported catalysts during hydrogenation of the mixture of styrene and phenylacetylene suggesting that styrene hydrogenation occurred on such catalysts.

4. Conclusions

It was revealed by XRD and XPS analysis that palladium silicide was formed on the sol–gel derived silica supported Pd catalysts prepared by ion-exchange method. However, such catalysts exhibited good performances in liquid-phase

semihydrogenation of phenylacetylene with highest styrene selectivity (~60%) at 100% conversion of phenylacetylene while the commercial SiO₂ supported ones exhibited no styrene selectivity. The specific activity of the catalysts was not affected by the formation of palladium silicide since the TOFs were essentially the same regardless of palladium silicide formation. They were rather influenced by the changes in palladium particle size since the TOFs decreases by an order of magnitude when palladium particle sizes were smaller than 3–5 nm.

Acknowledgments

Authors would like to thank the Thailand Research Fund (TRF), the Graduate School of Chulalongkorn University, and the Commission for Higher Education for the financial supports.

References

- [1] L. Guzzi, A. Horvath, A. Sarkany, *Stud. Surf. Sci. Catal.* 145 (2003) 351.
- [2] O. Dominguez-Quintero, S. Martinez, Y. Henriquez, L. D'Ornelas, H. Krentzien, J. Osuna, *J. Mol. Catal. A* 197 (2003) 185.
- [3] I. Palinko, *Appl. Catal. A* 126 (1995) 39.
- [4] T. Lopez, M. Asomoza, P. Bosch, E. Garcia-Figueroa, R. Gomez, *J. Catal.* 138 (1992) 463.
- [5] T. Nozoe, K. Tanimoto, T. Takemitsu, T. Kitamura, T. Harada, T. Osawa, O. Takayasu, *Solid State Ionics* 141 (2001) 695.
- [6] J.W. Park, Y.M. Chung, Y.W. Suh, H.K. Rhee, *Catal. Today* 93 (2004) 445.
- [7] N. Marin-Astorga, G. Pecchi, J.L.G. Fierro, P. Reyes, *Catal. Lett.* 91 (2003) 115.
- [8] D.V. Nadkarni, J.L. Fry, *J. Chem. Soc., Chem. Commun.* 12 (1993) 997.
- [9] G.L. Haller, D.E. Resasco, *Adv. Catal.* 36 (1989) 173.
- [10] W. Juszczuk, Z. Karpinski, D. Lomot, J. Pielaszek, *J. Catal.* 220 (2003) 299.
- [11] W. Juszczuk, D. Lomot, J. Pielaszek, Z. Karpinski, *Catal. Lett.* 78 (2002) 95.
- [12] A. Molnar, G.V. Smith, M. Bartok, *J. Catal.* 101 (1986) 67.
- [13] R. Tschan, R. Wandeler, M.S. Schneider, M. Burgener, M.M. Schubert, A. Baiker, *J. Catal.* 204 (2001) 219.
- [14] R. Tschan, R. Wandeler, M.S. Schneider, M. Burgener, M.M. Schubert, A. Baiker, *Appl. Catal. A* 223 (2002) 73.
- [15] T. Ichinohe, S. Masaki, K. Kawasaki, H. Morisaki, *Thin Solid Film* 343 (1999) 119.
- [16] R. Lamber, N. Jaeger, G. Schulz-Ekloff, *J. Catal.* 123 (1990) 285.
- [17] W. Juszczuk, Z. Karpinski, *J. Catal.* 117 (1989) 519.
- [18] W. Juszczuk, Z. Karpinski, J. Pielaszek, J.W. Sobczak, *New J. Chem.* 7 (1993) 573.
- [19] L. Kepinski, M. Wolcyrz, *Appl. Catal.* 73 (1991) 173.
- [20] B. Schleich, D. Schmeisser, W. Gopel, *Surf. Sci.* 191 (1987) 367.
- [21] A.J. Brunner, P. Oelhafen, H.-J. Guntherodt, *Surf. Sci.* 188 (1987) 1122.
- [22] A.J. Brunner, A. Stemmer, L. Rosenthaler, R. Wiesendanger, M. Ringer, P. Oelhafen, H. Rudin, H.-J. Guntherodt, *Surf. Sci.* 181 (1987) 313.
- [23] N. Marin-Astorga, G. Alvez-Manoli, P. Reyes, *J. Mol. Catal. A* 226 (2005) 81.
- [24] A. Molnar, A. Sarkany, M. Varga, *J. Mol. Catal. A* 173 (2001) 185.
- [25] D. Duca, L.F. Liotta, G. Deganello, *J. Catal.* 154 (1995) 69.
- [26] G. Carturan, G. Facchin, G. Cocco, S. Enzo, G. Navazio, *J. Catal.* 76 (1982) 405.
- [27] A. Sarkany, A.H. Weiss, L. Guzzi, *J. Catal.* 98 (1986) 550.
- [28] P. Albers, K. Seibold, G. Prescher, H. Muller, *Appl. Catal. A* 146 (1999) 135.
- [29] G. del Angel, J.L. Benitez, *J. Mol. Catal. A* 94 (1994) 409.